Preparation of a Novel Alloy Composed of Fluorene-Based Polyester and Polycarbonate and their Properties for the Optical Uses

Shinichi Kawasaki,[1] Masahiro Yamada,[1] Kana Kobori,[1] Hiroki Sakamoto,[1] Yoshikazu Kondo,[2] Fengzhe Jin,[2] Toshikazu Takata[3]

[1]*Department of Advanced Material Business Promotion, Osaka Gas Co., Konohana, Osaka 554-0051, Japan*
[2]*Advanced Materials Research Laboratory, KRI Incorporated, Shimogyo, Kyoto 600-8813, Japan*
[3]*Department of Organic and Polymeric Materials, Tokyo Institute of Technology, Meguro, Tokyo 152-8552, Japan*

Received 8 January 2008; accepted 28 May 2008
DOI 10.1002/app.28961
Published online 9 October 2008 in Wiley InterScience (www.interscience.wiley.com).

ABSTRACT: This paper is concerned with the structures and properties for fluorene-based polyester-polycarbonate (FBP/PC) alloys. Obtained alloys were characterized thermodynamically, optically, and viscoelastically, and the relationship between drawing behavior and molecular dynamics were also investigated. FBP/PC alloys showed transparent and a single glass transition temperature (*Tg*) for all compositions that indicated the complete compatibility in FBP/PC alloy systems. Tendency of the maximum draw ratios for alloy sheets was very similar to the profile of *Tg* versus FBP content. Maximum draw ratio was increased linearly with FBP content, demonstrating the intimate relationship between the large deformation and the molecular motion. A large amount of orientational birefringence occurred in PC sheet, but in the case of FBP/PC alloys and FBP, orientational birefringence was drastically decreased or not observed at all. This meant that positive birefringence of PC molecules was compensated by the absolutely smaller birefringence of FBP molecules. From a molecular mobility perspective, relaxation time (*T*2) for PC was smaller even at 200°C. However, for FBP and its alloys, *T*2 were much larger, showing the considerably enhanced molecular mobility in FBP or FBP/PC alloys. In this study, we could first reveal that the relationship between *Tg* and FBP content was very similar to the behaviors of birefringence (Δn)/draw ratio (λ) versus FBP content, *T*2 versus FBP content and 1/maximum draw ratio (λ_{max}) versus FBP content. Based on these results, we were able to propose a novel alloy with high refractive index, low orientational birefringence, and higher processability by alloying FBP with PC. © 2008 Wiley Periodicals, Inc. J Appl Polym Sci 111: 461–468, 2009

Key words: alloys; fluorene; PC; orientation; birefringence

INTRODUCTION

Fluorene-based polyester (FBP) with a "*cardo*" structure caused by 9,9-diarene-substituted fluorene skeleton has been recently focused upon as a promising polymer material for optical use because of its higher refractive index, lower orientational birefringence, higher glass transition temperature (*Tg*), and excellent transparency.[1–4] The optical property of some functional polymers with fluorene moieties has been also reported.[5–9]

Because of the "*cardo*" structure of FBP, the orientational birefringence induced by molding or drawing is difficult to be occurred, and this property is a significantly advantageous property in the optical field. Fine dispersions of nano-ordered inorganic fillers and certain other organic fillers in fluorene based polymers was also reported, as well as the fact that the "*cardo*" structure plays important roles in enhancing fine dispersion of the fillers in FBP.[10–13]

It is well known that polycarbonate (PC) is one of the typical heat resistant and transparent plastics and used in many optical fields owing to these features. However, on the other hand PC has the disadvantage of significant orientational birefringence. Improving this disadvantage, the molecular weight of PC resin used for compact discs or digital versatile discs, in which the significant birefringence is a fatal fault, must be decreased to reduce the orientational birefringence. As a result, the physical properties such as impact strength and heat resistance decline drastically, making it one of the bigger problems.

In this study, we studied the relationship between properties and structures of fluorene-based polyester-polycarbonate (FBP/PC) alloys, and as a result we could propose a novel FBP/PC alloy for optical use with many excellent properties, such as high refractive index and low orientational birefringence, and higher transparency and processability through alloying of FBP with PC.

Correspondence to: S. Kawasaki (skawa@osakagas.co.jp).

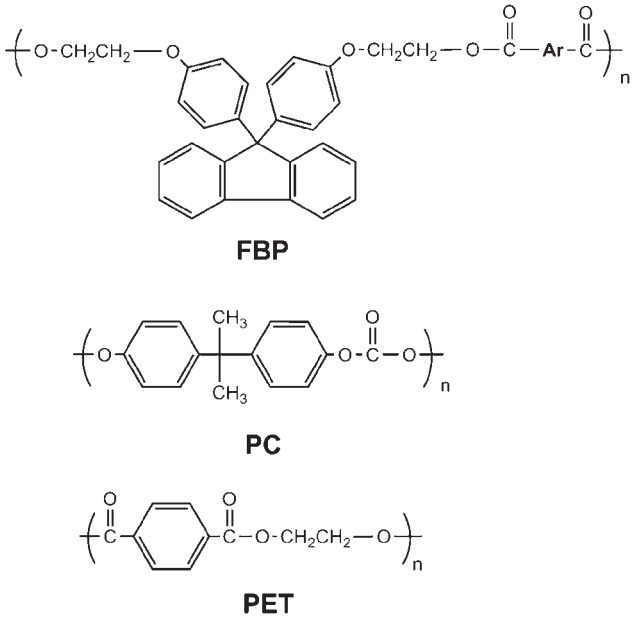

Scheme 1 Chemical structure of the materials used in this study; FBP, PC and PET from top to bottom.

EXPERIMENTAL

Materials

Fluorene based polyester (FBP-HX, Osaka Gas Chemicals, Japan), poly(carbonate) (PC, Panlite A1554, Teijin Chemicals, Japan) and poly(ethylene telephthalate) (PET, DIAPET MA 521, Mitsubishi Chemical Corp., Japan) were used without further purification. FBP, PC, and PET were dried in an air oven at 110°C for 12 h before hot processing. Chemical structures of FBP, PC, and PET are shown in Scheme 1.

Preparations of sheets of FBP/PC and PET/PC blends

A twin screw melt extruder KZW15-30MG (Technovel Co., Japan) was used to prepare the alloy of FBP/PC and form the alloy sheets through a T-die with 50 mm width and 1 mm clearance attached on the head of the extruder. Thickness of resulting sheets was controlled by being pressed between a pair of calender rolls. For alloying, FBP and PC were preblended and then fed into the extruder heated to 230–240°C, obtaining a sheet with 0.1 mm thickness. Sheets with various compositions of PET/PC blends were prepared in the same manner as above-mentioned.

Transparency measurement

Transparency of the obtained sheets with 0.1 mm thickness was measured using a UV-VIS Spectrophotometer UV3600 (Shimadzu Co., Japan) with an air window as a reference. In general, transparency of plastics is estimated by the cloud value at a light wavelength of 550 nm, and then transparency of sheets was estimated as the value obtained at a light wavelength of 550 nm in this study.

Thermal analysis

Glass transition temperature was measured using a differential scanning calorimeter (Thermo plus DSC 8230, Rigaku Co., Japan). For DSC measurement, each sample of about 3 mg was used and measured at the heating rate of 10°C/min. in a flow of N_2.

Viscoelastic measurement

For the viscoelastic measurement, drawn and undrawn sheets were cut into small pieces with 3 mm width and 50 mm length along the drawing direction. A viscoelastic measurement was performed to measure the storage modulus (E′), the loss modulus (E″), and the loss tangent value (tan δ) within the temperature range from room temperature to 260°C with the tensile mode at 100 Hz on a Rheogel-E4000 (UBM Ltd., Japan).

Drawing of sheets

An unstretched sheet was heated in an air oven of 140°C (for FBP), 145°C [for FBP/PC = 70/30 (w/w)], 150°C [for FBP/PC = 50/50 (w/w)] at 155°C (for PC) for 3 min., and then immediately drawn at the same temperature at a drawing rate of 500%/min. by a drawing machine TYPE HW-500 (Oba machinery Co.). The draw ratio was calculated by the following eq. (1):

$$\lambda_d = l/l_0 \tag{1}$$

where λ_d, l_0 and l represent the draw ratio and the initial distance of the neighboring points marked on the sheet before and after drawing, respectively.

Measurement of the birefringence

The orientation behavior in the sheet was observed by inserting the drawn sheet into the two crossed polarized films. The birefringence of the drawn sheets was examined to measure the retardation (Re) in the sheet by a polarized-light microscope (OPTIPHOT-POL by NIKON, Japan). The value of birefringence was calculated as the following eq. (2):

$$\Delta n = \mathrm{Re}/d \tag{2}$$

where Δn, Re and d mean the birefringence, Re and thickness of the sheet, respectively.

The orientational birefringence for the drawn sheets was calculated by the following eq. (3):

$$\text{orientational birefringence} = \Delta n/\lambda_d \tag{3}$$

Wide angle X-ray diffraction observation

Drawn or undrawn sheets were cut into small pieces with 2 mm width and 20 mm length along the drawing direction for the wide angle X-ray diffraction observation (WAXD). Each piece was placed on a sample holder with its drawing direction perpendicular to the X-ray beam and the measurement was performed from 0 to 50° of its 2θ scanning angle on the WAXD instrument (Shimadzu XD-1, Japan).

Nuclear magnetic resonance measurement

Mobility of polymer molecules in the sheet sample was estimated using the spin-echo method and relaxation time (*T*2) by the solid state proton nuclear magnetic resonance (NMR) (1H NMR;JNM-MU25, JEOL, Japan). Measurement was performed at room temperature and at 100, 120, 140, 160, 180, and 200°C to investigate the temperature dependence of molecular motion.

RESULTS AND DISCUSSIONS

Transparency of FBP/PC alloys

The values of transparency for the obtained FBP, PC and their alloy sheets are summarized in Table I. The alloy sheets of FBP/PC had excellent transparency over all blending ratios. On the other hand, PET/PC blends were opaque, apparently because of the phase separation between PET and PC, as shown in Figure 1. These results clearly demonstrate that FBP/PC alloy system is absolutely compatible and miscible, whereas conversely, PET/PC alloys are completely immiscible and incompatible.[14–15]

Glass transition temperature

The observed *Tg* values for FBP/PC alloys are demonstrated in Figures 2 and 3 and Table II. *Tg* values straightly decrease with an increase in FBP content, as shown in above figures, which means that the molecular mobility in alloys is actually related with FBP content in alloys. It must be noted that FBP content dependencies of *Tg* obtained by DSC are very similar to the behaviors of tan δ versus temperature, $1/\lambda_{max}$ versus FBP content, and $\Delta n/\lambda$ versus FBP content as mentioned below.

TABLE I
Transmittances of Light at 550 nm for Sheets Obtained With 0.1 mm Thickness

Sample	T_{550} (%)
FBP	94.0
FBP/PC = 70/30	96.8
FBP/PC = 50/50	95.6
PC	93.3

Viscoelastic properties

Figure 4(A,B) show the tan δ behaviors against temperature for FBP, PC, PET and their respective blends. In FBP/PC alloys, a single tan δ was observed in all compositions, because these two polymers are miscible and formed a homogeneous phase with single glass transition. This represents obvious evidence for the high compatibility of FBP with PC, because not only the intermolecular interaction through π–π interaction between fluorene groups of FBP and phenyl groups of PC, but also the higher free volume because of the "*Cardo*" structure in FBP. On the other hand, in the case of PET/PC alloys, two tan δ peaks related to each component could be apparently observed to represent the phase separation between them. The intermolecular interaction between PET and PC was considered weak to generate a compatible alloy of the two different polymers, resulting in two separated tan δ peaks as shown in Figure 4(B).

Drawing behavior

FBP sheet was easily drawn up to the highest draw ratio over 25 times of the original sheet, as shown in Figure 5. λ_{max} indicates the maximum draw ratio;

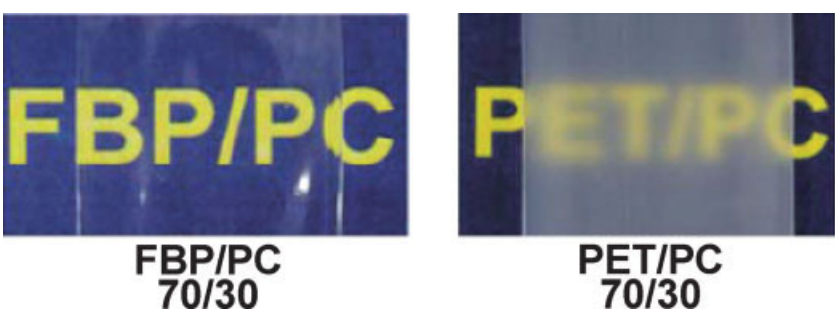

Figure 1 Photographs of alloy sheets located on the paper: FBP/PC alloy (left) and PET/PC alloy (right). It is apparent that FBP/PC alloy is quite transparent compared with PET/PC alloy. [Color figure can be viewed in the online issue, which is available at www.interscience.wiley.com.]

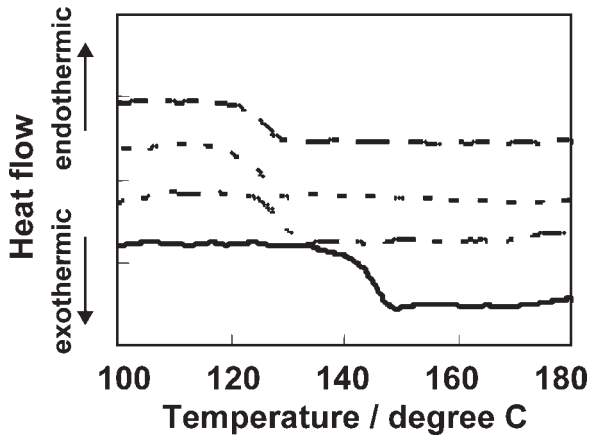

Figure 2 Observed DSC curves for FBP/PC = 100/0 (dashed line), 70/30 (dot line), 50/50 (dash-dot line) and 0/100 (solid line).

defined as the draw ratio at breaking point by the drawing process.

The drawing mechanism of polymer materials is generally considered to be caused by unentanglement or sliding of the molecules. Hence, $1/\lambda_{max}$ can be considered to be one of the measures for the molecular mobility. Figure 5 shows the relationship between $1/\lambda_{max}$ and FBP content. With FBP content (0 to 70 wt %), $1/\lambda_{max}$ is linearly decreased with increasing FBP content, and almost constant over 70 wt % FBP content. Because of the alloying of FBP and PC the maximum draw ratio (λ_{max}) is increased from 2 to 3 times for a PC sheet to 20 times for FBP/PC alloy containing 70 wt % FBP, and 7.5 times for FBP/PC alloy containing 50 wt % FBP, respectively.

The profile of this figure is very similar to that of DSC-profile or NMR-profile. Based on these results, it was first revealed that the molecular motion of PC and FBP in alloys is directly related to large deformation such as drawing.

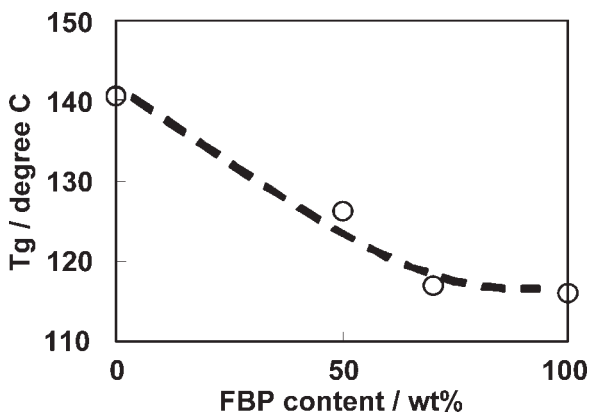

Figure 3 Relationship between *Tg* and FBP content. *Tg*'s values decrease linearly up to 70 wt % of FBP content in alloys, but are almost constant from 70 to 100 wt % of FBP content.

TABLE II
Glass Transition Temperatures (*Tg*) Measured for FBP, FBP/PC Alloy and PC by DSC

Sample	Tan δ/°C
FBP	132.0
FBP/PC	136.5
PC	149.8
PET	80.3
PET/PC	73.3/147.3

The mechanical, thermal, and optical properties are dependent on the processing conditions such as drawing; consequently, the large draw ratio for FBP/PC alloy sheets is a very important factor for film processability and properties from the view point of industrial stage.

Birefringence

Figure 6 is an optical photograph of the Re behaviors of the drawn sheets inserted into the crossed-polarized films. This photograph indicates that the drawn PC sheet had strong and apparent Re. On the other hand, for FBP drawn sheet no Re could be

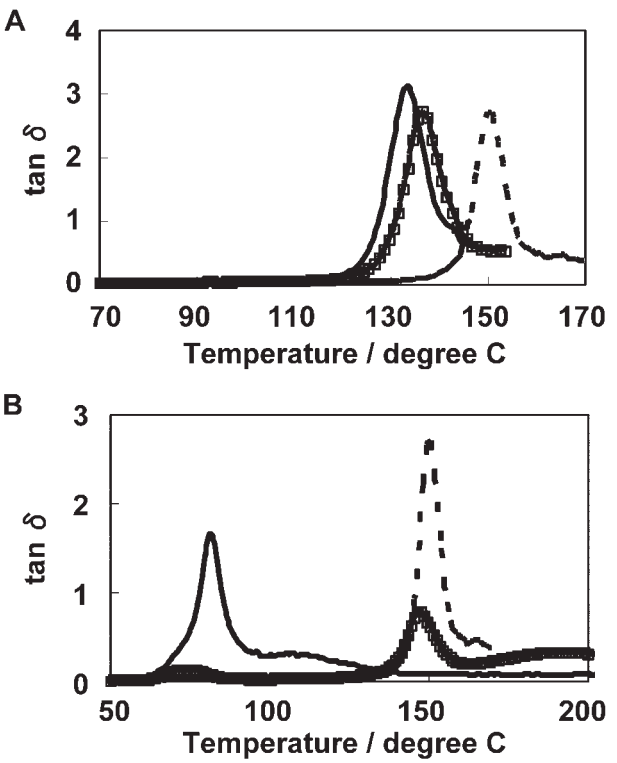

Figure 4 Tan δ charts plotted against the observed temperature by the viscoelastic measurement for FBP (solid line), PC (dashed line) and FBP/PC alloy systems in Figure A and PET (solid line), PC (dashed line) and PET/PC alloy systems in Figure B. Only one peak of tan δ is observed in each FBP/PC alloy; however, the two peaks because of each component of the alloy are observed in PET/PC alloy system.

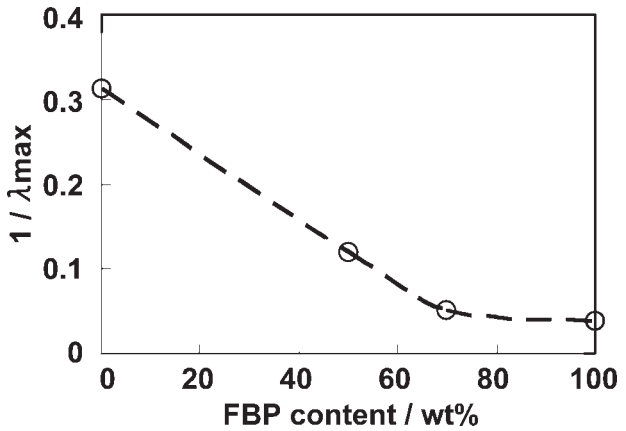

Figure 5 Maximum draw ratios (λ_{max}) of PC, FBP and their alloys. The values of $1/\lambda_{max}$ decrease straightly up to 70 wt % of FBP content in alloys but are almost constant over 70 wt % of FBP content.

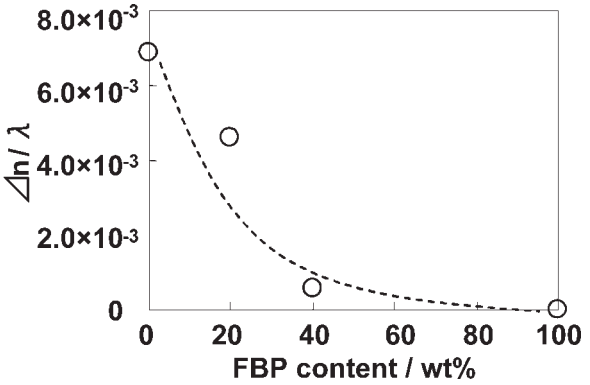

Figure 7 Relationship between the orientational birefringence ($\Delta n/\lambda$) and FBP content in alloy sheets. The values of $\Delta n/\lambda$ largely decrease up to 40% of FBP content in alloy sheets but remain almost constant from 40 to 100 wt % of FBP content.

observed, while a small amount of Re was occurred for FBP/PC alloys. These resulting birefringence values are much smaller than that of PC. Here, the alignment of the fluorene groups on the side chain of FBP polymer on the same planes is considered to be difficult, and then it consequently results in decreasing in the orientational birefringence induced by drawing. The strength of the birefringence is one of the key factors for the quality in the optical use as mentioned above.

The values of the orientational birefringence are defined by the following eq. (3):

$$\text{orientational birefringence} = \Delta n/\lambda_d \qquad (3)$$

where Δn and λ indicate the birefringence and the draw ratio, respectively.

The orientational birefringence in the drawn FBP sheet could not be observed because of the molecular structure characterized by the bulky fluorene group located perpendicular to the main chain in FBP, known as the "*Cardo*" structure. On the other hand, the two benzene rings combined in parallel to the main chain in PC are easily orientated to induce the larger birefringence by drawing. Figure 7 indicates the relationship between the birefringence and FBP content for the drawn sheets. It apparently shows that $\Delta n/\lambda = 7 \times 10^{-3}$ for PC is much larger than ones for FBP and FBP/PC alloys. This lower orientational birefringence for alloys can be considered to be occurred as follows. The positive birefringence in PC molecules is compensated for by the far smaller birefringence in FBP molecules because of the complexation of PC and FBP molecules in the alloys. The driving force of such complexation is considered to be due to the intermolecular interaction through π–π interaction between PC and FBP or the higher free volume in FBP molecule. These results apparently demonstrate that the molecules of both PC and FBP move cooperatively during deformation, and the relationship between Δn and FBP content is very similar to the relationships between *Tg* and FBP content, *T*2 and FBP content and $1/\lambda_{max}$ and FBP content.

This work could first reveal that the alloy of FBP and PC achieved excellent miscibility and transparency, and lower orientational birefringence, and it had the

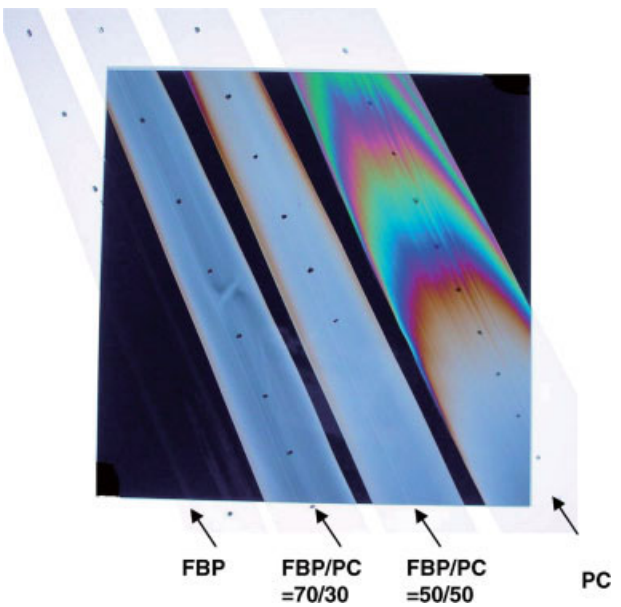

Figure 6 Photograph of the retardation observed in the drawn sheets of FBP, FBP/PC alloys and PC (from left to right) located between two crossed polarized films. For FBP sheet the retardation can not be observed because of no retardation; however, in PC sheet, apparent interferences are observed owing to the significant retardation induced. [Color figure can be viewed in the online issue, which is available at www.interscience.wiley.com.]

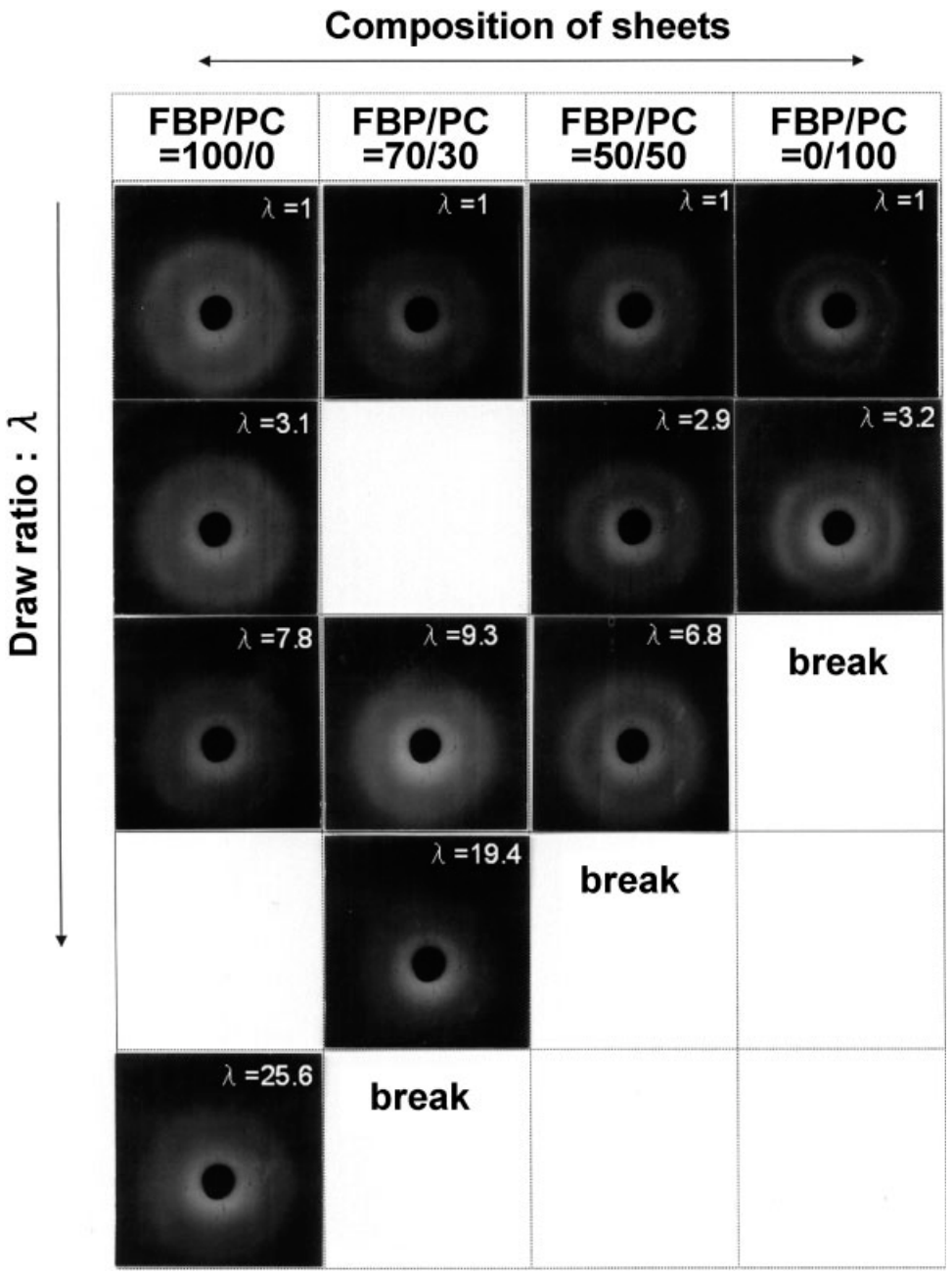

Figure 8 Photographs of the WAXD for PC and FBP/PC alloy (50/50). None or extremely weak amorphous and unoriented halo patterns but some regular structures are observed in drawn PC.

significant advantages for the optical use of PC related materials. The orientational birefringence induced by injection, extruding or drawing processes is one of the biggest problems for PC. In general, to decrease the orientational birefringence of PC, the molecular weight must be decreased and as a result the physical properties of PC products decline significantly.

However, results of this study demonstrated that a high molecular weight PC could be used for the optical purposes, thanks to the extraordinarily lower orientational birefringence by alloying with FBP. Consequently, the physical and thermal properties of the molded products could be improved, which may also improve the possibilities and properties of the devices or products in the optical field.

Wide angle X-Ray diffraction

No orientation patterns were observed in WAXD patterns for the undrawn sheets of FBP, PC, and FBP/PC alloys, whereas for PC drawn sheets, the halo ring was split into four patterns owing to the incidence of amorphous orientation with the increasing draw ratio as shown in Figure 8. However, for

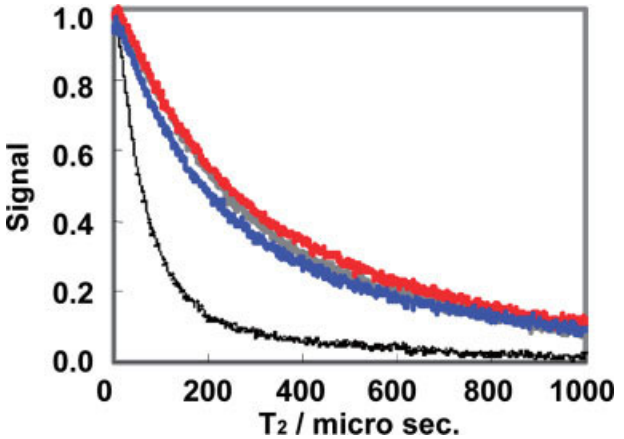

Figure 9 NMR signal decay curves against the relaxation time *T*2 for FBP (red line), PC (black line), FBP/PC = 50/50 (w/w) alloy (sky blue line), and FBP/PC = 30/70 (w/w) alloy (blue line), respectively. [Color figure can be viewed in the online issue, which is available at www.interscience.wiley.com.]

the drawn FBP and FBP/PC alloy sheet, no special orientation patterns were observed, even at the higher draw ratio. These results suggest that PC is easily able to generate some regular structure under the hot drawing, but its tendency is weakened by alloying with FBP. Easy crystallization of PC by thermal annealing is one of the disadvantages for PC. However, the crystallization tendency was drastically restrained by alloying with FBP and then it reduced the crystallization tendency for PC. These results indicate the high compatibility between FBP and PC. It seems to be because of the interaction between PC and FBP molecules via π–π or CH–π interaction. Reduced crystallization property for PC is a great advantage in the optical material field.

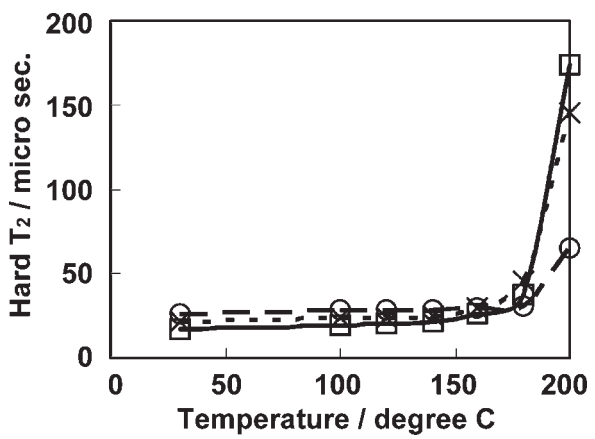

Figure 10 Relationship between the relaxation time *T*2 and the observed temperature: *T*2 of PC (open circle and dashed line) is much smaller than those for FBP (open rectangular and solid lines) and FBP/PC alloy (cross and dotted line). This means that the molecular motion of PC is much smaller than those of FBP and FBP/PC alloy.

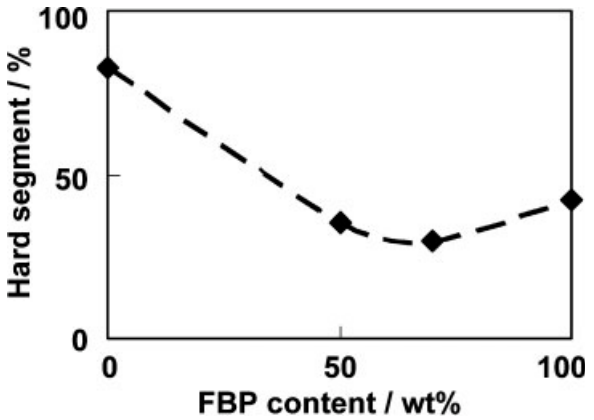

Figure 11 Relationship between the hard segment and FBP content: the fractions of the hard segment are decreasing up to 70 wt % of FBP content in alloy. These show that FBP component in alloys can enhance the molecular mobility in the same. This relationship is very similar to those of *Tg* behavior (Fig. 3) and 1/λ behavior (Fig. 5).

Solid state NMR measurement of FBP/PC alloy

Spin-spin relaxation time *T*2's analyzed from free induction decay signals for FBP, PC and their alloys against temperature are demonstrated in Figure 9. It is generally well known that *T*2 is strongly related to the mobility of molecules. The longer the relaxation time *T*2, the easier the molecular motion. For PC, *T*2 is not large, even at elevated temperatures up to 200°C, showing that the molecular motion of PC is poor. On the other hand, it was apparently demonstrated that for FBP and FBP/PC alloys, the mobility of molecules was more active at 150°C and higher. At 200°C, FBP had a relaxation time (*T*2) of 150 μs, which was much higher than the time for PC. By alloying PC with FBP, *T*2 was increased drastically and reached a level equivalent to almost the same values for FBP, as shown in Figure 10. This means that the mobility of PC molecules was increased by alloying with FBP, and the high miscibility and compatibility of FBP and PC enabled to enhance the mobility of PC because of the cooperative molecular motion. Figure 11 shows the hard segmental fraction against FBP content. The hard segment fraction is one of the measures of molecular mobility. This figure clearly indicates that PC has an amount as large as 80%, and that this fraction is decreasing with increasing FBP content. These results indicate that the mobility of PC will be enhanced by alloying with FBP.

CONCLUSIONS

FBP/PC alloys studied in this report have the excellent optical transparency and single glass transition temperature, and as a result it strongly

demonstrated the complete miscibility and compatibility in the alloys. For the processability of alloy sheets, FBP sheet could be drawn up to the maximum draw ratio (λ_{max}) of 24, which was about 7 times larger than that of PC. The values of λ_{max} for FBP/PC alloys were strongly dependent on FBP content. One of the great advantages for the present alloys is that the orientational birefringence is much smaller than PC, because the induced positive birefringence in PC molecules is compensated by the much smaller birefringence because of the "*cardo*" structure in FBP molecules.

FBP has a high molecular mobility compared to that of PC, hence, it can significantly enhance the mobility of PC molecules in FBP/PC alloys, because PC and FBP are completely compatible to each other and move cooperatively in FBP/PC alloys.

Based on the above results, we were first able to reveal that the relationship between *Tg* and FBP content was very similar to the behaviors of $\Delta n/\lambda$ versus FBP, *T*2 by NMR versus FBP and $1/\lambda_{max}$ versus FBP. As a result, we could propose a novel FBP/PC alloy for optical use with many excellent properties, such as high refractive index and low orientational birefringence, and higher transparency and processability through alloying of FBP with PC.

References

1. Inoue, T.; Fujiwara, K.; Ryu, D. S.; Osaki, K.; Fuji, M.; Sakurai, K. Polym J 2000, 32, 411.
2. Sakurai, K.; Fuji, M. Polym J 2000, 32, 676.
3. Uchiyama, A.; Yatabe, T. J Polym Sci Part B Polym Phys 2003, 41, 1554.
4. Persson, N. K.; Arwin, H.; Inganas, O. J. Appl Phys 2005, 97, 034503.
5. Okamura, H.; Sakai, K.; Tsunooka, M.; Shirai, M.; Fujiki, T.; Kawasaki, S.; Yamada, M. J Photopolym Sci Tech 2003, 16, 87.
6. Tokumitsu, K.; Tanaka, A.; Kobori, K.; Kozono, Y.; Yamada, M.; Nitta, K. J. Polym Sci Part B Polym Phys 2005, 43, 2259.
7. Tokuhisa, K.; Hamada, E.; Karinaga, R.; Shimada, N.; Takeda, Y.; Kawasaki, S.; Sakurai K. Macromolecules 2006, 39, 9480.
8. Kawasaki, S.; Yamada, M.; Kobori, K.; Jin, F. Z.; Kondo, Y.; Hayashi, H.; Suzuki, Y.; Takata, T. Macromolecules 2007, 40, 5284.
9. Seesukphronrarak, S.; Kawasaki, S.; Kobori, K.; Takata, T. J Polym Sci Part A Polym Chem 2007, 45, 3073.
10. Inada, T.; Masunaga, H.; Kawasaki, S.; Yamada, M.; Kobori, K.; Sakurai, K. Chem Lett 2005, 34, 524.
11. Matsukawa, K.; Matsuura, Y.; Nakamura, A.; Nishioka, N.; Murase, H.; Kawasaki, S. J Photopolym Sci Technol 2007, 20, 307.
12. Kawasaki, S.; Yamada, M.; Kobori, K.; Kakumoto, T.; Jin, F. Z.; Tarutani, A.; Takata, T. Polym J 39: 115 2007.
13. Kawasaki, S.; Yamada, M.; Kobori, K.; Kakumoto, T.; Jin, F. Z.; Takata, T. Polym Comp 2008, 29, 1024.
14. Takeshima, M.; Funakoshi, N. J Appl Polym Sci 1987, 32, 3457.
15. Saffell, J. R.; Windle, A. H. J Appl Polym Sci 1980, 25, 1117.